Proc. Int. Symposium on Advances in Neutron Scattering Research, Tokai, 2000
J. Phys. Soc. Jpn. **70** (2001) Suppl. A pp. 534–536

Residual Strain Measurement of an Unidirectionally Solidified Al_2O_3/YAG Composite by TOF Neutron Diffraction

Syuuki TORII, Tomohiro TOYA, Takashi KAMIYAMA[1], Yoshiharu WAKU[2], Hajime ASANO, Toshiharu FUKUNAGA[3]

Institute of Materials Science, University of Tsukuba, Ibaraki 305-8573, Japan
[1]*High Energy Accelerator Research Organization, Ibaraki 305-0801, Japan*
[2]*Japan Ultra-high Temperature Materials Research Institute, Yamaguchi 755-0001, Japan*
[3]*Research Reactor Institute, Kyoto University, Osaka 590-0494, Japan*

Residual stresses are responsible for unexpected destruction of structures due to fatigue failures or stress corrosion cracking. Neutrons evidently penetrate deep into the components, and then have the potential for a major breakthrough in this field. In this study, neutron residual strain measurements were carried out with a high-resolution time-of-flight diffractometer *Sirius* at KENS for the unidirectionally solidified $Al_2O_3/Y_3Al_5O_{12}$ (YAG) composite. For the measurement of this composite material, we developed a new technique combining the Laue patterns and high-resolution TOF data. Using this technique, we succeeded in the detailed indexing of the Laue pattern, and decided azimuthal relation of the Al_2O_3 phase and the YAG phase. Then it was found that YAG was in tension state and Al_2O_3 under compression in composite Al_2O_3/YAG.

KEYWORDS: residual strain, time-of-flight, neutron diffraction, Al_2O_3/YAG

§1. Introduction

Unidirectionally solidified Al_2O_3/YAG eutectic composite was developed by controlling the solidification process.[1–3] The eutectic composite has a new microstructure, in which single crystal Al_2O_3 and single crystal YAG are three-dimensionally and continuously connected and finely entangled without grain boundaries. This eutectic composite material attracts attention recently, since bending strength and thermal stability at high temperature are more excellent than conventional ceramic materials. The reason of the high temperature characteristic is closely related with the absence of grain boundaries, which generally degrade the stability and weaken the strength at high temperature. It is noted that the absence of the grain boundaries might be ascribable to the single crystalline nature of the composite material. However, the high-strength mechanism of this composite material at high temperature is not very much understood.

In this study, residual strain measurements of eutectic composite material of Al_2O_3 and YAG were carried out with the TOF-Laue method using a neutron diffractometer *Sirius* at KEK.[4,5] The method combining the Laue patterns and TOF data is established and applied for the first time.

§2. Experimental

The residual strain measurement with TOF-Laue method is based on the Bragg's law:

$$2d\sin\theta = \lambda \qquad (1)$$

where λ is neutron wavelength, d lattice plane spacing, and θ scattering angle. When d changes from d^0_{hkl} to d_{hkl} by elastic strain, the residual strain quantity ϵ_{hkl} is defined as follows:

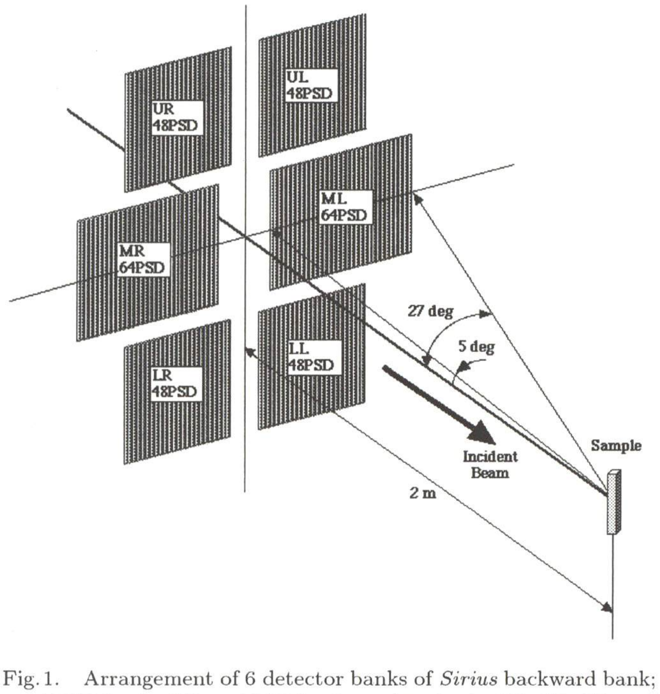

Fig. 1. Arrangement of 6 detector banks of *Sirius* backward bank; 64 PSD in the ML and MR banks and 48 in the LL, LR, UL and UR banks have been installed.

$$\epsilon_{hkl} = \frac{d_{hkl} - d^0_{hkl}}{d^0_{hkl}} \qquad (2)$$

where d^0_{hkl} is d-spacing without strain. In this work, the value of d^0_{hkl} was obtained by the separate measurement on polycrystal samples. We used the backward bank of *Sirius*, in which 60% of 500 one-dimensional po-

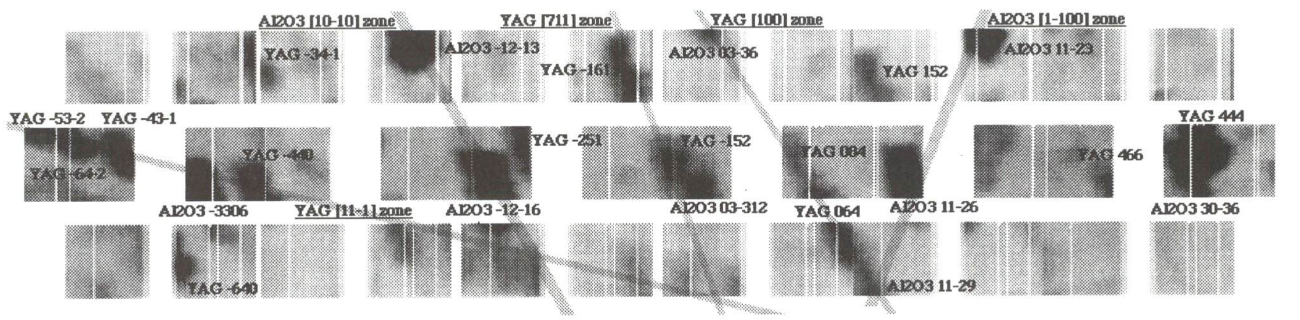

Fig.2. Laue patterns by *Sirius* backward bank: superimposed six Laue patterns. Between successive Laue patterns, the specimen is rotated by 20° around the vertical axis.

sition sensitive detectors (PSD) have been already installed; 6 detector banks at the backward is situated at 2m apart from a sample position (Fig. 1). The scattering angle in horizontal plane is $2\theta = 153° \sim 175°$. The number of position pixels amounts to over 80 thousand. Then TOF-Laue diffractometry with wide range of 2θ and wavelength ($\lambda = 0 \sim 5$Å) is possible.

The used samples are unidirectional solidified eutectic composite material Al_2O_3/YAG, sintered polycrystal Al_2O_3 and sintered polycrystal YAG. The composite Al_2O_3/YAG was manufactured by heating an ingot at 2223 K, followed by cooling at a speed of 5mm/h. In the composite material, single crystal Al_2O_3 and YAG, with the molar ratio of about 52 : 12, are three-dimensionally and continuously connected each other. The dimensions of the composite Al_2O_3/YAG, the sintered Al_2O_3 and the sintered YAG were $5 \times 5 \times 50$ mm^3, and the long axis of the specimen was set vertical. The several sets of TOF-Laue patterns were measured for about 90 minutes before rotating 20° around the vertical axis and six horizontally sequential TOF-Laue patterns were obtained. Conventional Laue patterns were easily obtained by integrating over TOF axis. Each conventional Laue pattern as horizontally superimposed and shown in Fig.2.

Bragg peaks in Laue patterns are found to be broad and severely overlapped. In such cases, the angle dispersive diffractometers are not suited for the precise evaluation of the residual strain. In TOF-Laue diffractometry, on the other hand, we can sum up all TOF pattern from a selected Bragg spot. Because precise evaluation of the residual strain is indispensable, Bragg reflections of polycrystal Al_2O_3 and YAG were also accumulated in the same region as that used in the Al_2O_3/YAG composite. It is noted that indexing reflections in a duplicated Laue pattern is easy since *Sirius* is a high-resolution TOF diffractometer, and this step is necessary in the precise measurements of d-spacings of eutectic composite materials. The values of d_{hkl} and d^0_{hkl} were determined by the least square fitting for summed Bragg reflections of Al_2O_3/YAG and polycrystals, respectively. The value of ϵ_{hkl} is obtained from eq.(2).

§3. Result and Discussion

3.1 *TOF-Laue pattern of Al_2O_3/YAG*

The $\bar{4}40$, $\bar{1}52$ and 444 Bragg spots of YAG in horizontal plane shown in Fig. 2, belong to $[11\bar{2}]$ zone, which indicates the crystal orientation is $11\bar{2}$ along the long axis of the specimen. This is consistent with other Bragg spots of YAG; the $\bar{5}3\bar{2}$, $\bar{6}4\bar{2}$, $\bar{4}3\bar{1}$ and $\bar{4}40$ reflections belong to the $[11\bar{1}]$ zone and the 084 and 064 to the [100] zone. Similarly, the $11\bar{2}3$ and $11\bar{2}6$ Bragg spots in the Al_2O_3 phase, belong to the $[1\bar{1}00]$ zone. All other Bragg spots are consistently indexed. The crystal orientation of Al_2O_3 along the long axis of the specimen is close to $02\bar{2}\bar{5}$.

The Laue spots of both phases are severely broadened. For example, the Laue spot of the $\bar{1}61$ reflection of the YAG phase has a shape of ellipse with $10° \times 3°$.

Table I. The d-spacing and ϵ_{hkl} for sintered YAG, sintered Al_2O_3 and composite Al_2O_3/YAG.

	reflection index hkl	d-spacing [Å] Al_2O_3/YAG composite	Al_2O_3 sintered	YAG sintered	ϵ_{hkl} [$\times 10^{-4}$]
Al_2O_3 phase	$\bar{3}\ 3\ 0\ 6$	1.16028	1.16041		-1.12
	$1\ 1\ \bar{2}\ 9$	1.23485	1.23510		-2.02
	$1\ 1\ \bar{2}\ 6$	1.60198	1.60223		-1.56
	$2\ 0\ \bar{2}\ 4$	1.74051	1.74076		-1.44
	$\bar{1}\ 2\ \bar{1}\ 3$	2.08643	2.08689		-2.20
YAG phase	$\bar{6}\ 4\ \bar{2}$	1.60559		1.60514	2.80
	$4\ 4\ 4$	1.73406		1.73375	1.79
	$\bar{5}\ 3\ \bar{2}$	1.94865		1.94863	0.10
	$\bar{4}\ 4\ 0$	2.12387		2.12367	0.94
	$\bar{2}\ 5\ 1$	2.19308		2.19298	0.46
	$\bar{4}\ 3\ \bar{1}$	2.35633		2.35570	2.67

3.2 *Single peak fitting*

After adding the TOF data of each Bragg spot which appeared in the Laue pattern, the d-spacings of the composite material Al_2O_3/YAG, polycrystal Al_2O_3 and YAG were compared. TOF of each reflection was converted to d-spacing and several Bragg reflections are shown in Fig. 3, where Bragg peak was fitted with the profile function of *Sirius*. The value of d for each reflection was thus calculated. Parts of obtained values of d and ϵ_{hkl} are listed in Table I. The index of corresponding reflections are shown in Fig. 2. In both phases of Al_2O_3/YAG, the order of magnitude of ϵ_{hkl} was as small as 10^{-4}. All the values of ϵ_{hkl} in the Al_2O_3 phase were found to be negative while those in YAG positive. This result was confirmed by other 40 equivalent reflections,

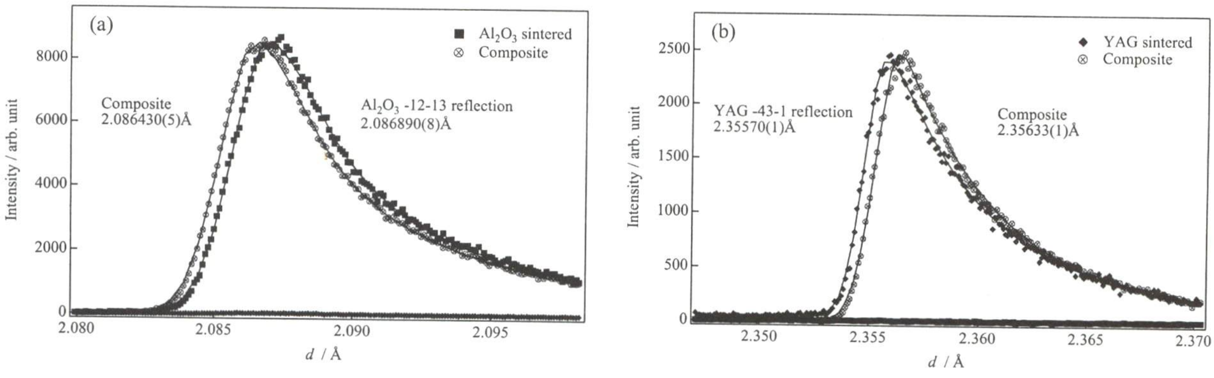

Fig. 3. Bragg peak of Al_2O_3 and YAG: (a) $\overline{1}2\overline{1}3$ reflection of Al_2O_3, (b) $\overline{4}3\overline{1}$ reflection of YAG.

which are not listed in Table I. Therefore, we can safely conclude that the Al_2O_3 phase is under compression and the YAG phase under tension.

3.3 Residual strain models

The 444 reflection of the YAG phase and the $30\overline{3}6$ reflection of the Al_2O_3 phase appear in the almost equal position. The $20\overline{2}4$ reflection of Al_2O_3, which is parallel to and appears at the position close to the $30\overline{3}6$ reflection, can be identified in TOF diffraction pattern. The d value is 1.740510(8)Å, while that of the 444 reflection of YAG is 1.734060(4)Å. Therefore, the d values and the position in the Laue pattern of 444 (YAG) and $20\overline{2}4$ (Al_2O_3) agree each other. This fact is of great interest in clarifying the mechanism of high-strength in Al_2O_3/YAG. In the reference polycrystal samples, d-spacing of the $20\overline{2}4$ reflection of Al_2O_3 is 1.74076(1)Å, and d-spacing of 444 reflection of YAG is 1.73375(2)Å. Compared these d values with those in Al_2O_3/YAG, we found the difference in the d-spacings of $20\overline{2}4$ (Al_2O_3) and 444 (YAG) were adjusted to be reduced in Al_2O_3/YAG. This might explain why the Al_2O_3 is under compression and the YAG under tension.

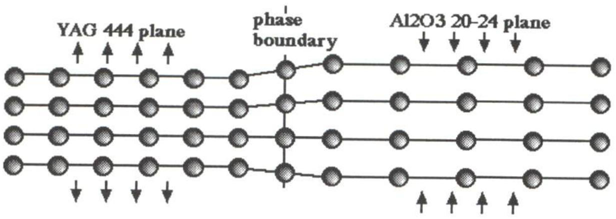

Fig. 4. A model (A) of Al_2O_3 and YAG phase boundary.

Presently, information on the grain boundaries is not available. Then we cannot explain how two d-spacings in both phases are adjusted. We speculated two models with different boundaries as shown in Figs. 4 and 5. In Fig. 4, two reflection planes contact at the two-phase boundary, because this composite material has the structure which intertwines without the crystal grain boundary. The 444 reflection plane of the YAG phase is pulled by the $20\overline{2}4$ reflection plane of Al_2O_3, resulting in the tension condition. Reversely, the Al_2O_3 phase is compressed by the YAG phase.

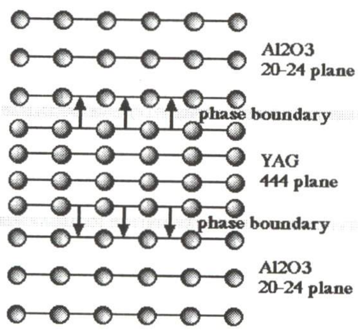

Fig. 5. A model (B) of Al_2O_3 and YAG phase boundary.

In the model (B), two planes might be stacked as shown in Fig. 5. In this model, it is assumed that, during the solidification process, the magnitude of shrink in the YAG phase is larger than that in the Al_2O_3. This model also explains why YAG is in tension state and Al_2O_3 under compression. In order to verify the validity of these models, information on the phase boundaries and detailed analysis of Bragg spot shapes are indispensable. In addition, temperature variations of thermal expansion are necessary.

In conclusion, the residual strain of eutectic composite Al_2O_3/YAG was observed in this measurement: the Al_2O_3 phase was in the compressional state and the YAG phase was in the tension state, and the order of magnitude of strain was 10^{-4}. Residual strain measurement of single crystal composite material using the TOF-Laue method is the very epoch-making technique which can analyze the crystal orientation relation and the strain amount.

1) Y. Waku, N. Nakagawa, H. Ohtsubo, Y. Ohsora and Y. Kohtoku: J. Japan. Inst. Materials **59** (1995) 71.
2) Y. Waku, N. Nakagawa, T. Wakamoto, H. Ohtsubo, K. Shimizu and Y. Kohtoku: Nature **389** (1997) 49.
3) Y. Waku, N. Nakagawa, T. Wakamoto, H. Ohtsubo, K. Shimizu and Y. Kohtoku: J. Mater. Science **33** (1998) 1217.
4) S. Torii, T. Kamiyama, K. Mori, K. Oikawa, S. Itoh, M. Furusaka, S. Satoh, S. Ikeda, F. Izumi and H. Asano: J. Phys. Chem. Solids **60** (1999) 1583.
5) T. Kamiyama, S. Torii, K. Mori, K. Oikawa, S. Itoh, M. Furusaka, S. Satoh, T. Egami, F. Izumi and H. Asano: Materials Science Forum **321-324** (2000) 302.